RESEARCH ARTICLE

Electrochemical, Kinetic, Antimicrobial (MIC) Studies of Acyclic Schiff-Base Nickel(II) Complexes†

S. PRAVEEN KUMAR[a], A.VIJAYARAJ[a], L. VIJAYALAKSHMI[b] and V. NARAYANAN[a*]

[a]Department of Inorganic Chemistry, University of Madras, Guindy Campus, Chennai-600025, India
[b]Vidhya Sagar Women's College, Chengalpattu, Kancheepuram-603211, India
vnnara@yahoo.co.in

Abstract: A series of acyclic mononuclear nickel(II) complexes have been prepared by Schiff base condensation derived from 5-bromosalicylaldehyde, diethylenetriamine, tris(2-aminoethyl) amine, triethylenetetramine, *N,N*-bis(3-aminopropyl)ethylene diamine, *N,N*-bis(aminopropyl) piperazine, nickel perchlorate. Electronic spectra of nickel(II) complexes show d-d transition in the range of 780-920 nm. Electrochemical studies of the nickel(II) complexes show irreversible one electron reduction, oxidation process. The reduction potential of the mononuclear nickel(II) complexes shifts towards anodic direction and oxidation potential shift towards to more cathodic direction upon increasing the chain length of the imine compartment. Electrochemical and catalytic studies of the complexes were compared on the basis of increasing the chain length of the imine compartment. All the complexes were screened for antifungal and antibacterial activity. Nickel is recognized as an essential trace element for bacteria, plants and animals. The active sites of enzymes such as urease, carbon monoxide dehydrogenase, [NiFe]-hydrogenase and methyl-*S*-coenzyme-M methylreductase are known to contain nickel centres, which are intimately involved in the catalytic cycles.

Keywords: Electrochemical, Kinetics, Antimicrobial studies, Acyclic Schiff-Base

Introduction

There has been a considerable effort in recent years towards the preparation of new Schiff base synthesized from the reaction of dialdehydes and amino compounds[1]. New Schiff base macroligands have been synthesized to study their selectivity towards complexation of metal ions. Schiff bases containing acyclic and cyclic imine bonds are of great importance in modern coordination chemistry[2]. Metal complexes of these ligands are widely used as luminescent complexes[3], liquid crystal[4] structures, chemosensors[5] and other useful metal-containing azomethine compounds[6]. Many transition metal ions in living systems work as enzymes or carriers in a macrocyclic ligand environment. Meaningful research in this direction might generate simple models for biologically occurring metalloenzymes[7] and thus help in further understanding biological systems. Nickel is recognized as an essential trace element for bacteria, plants and animals[8]. The active sites of enzymes such as urease, carbon monoxide dehydrogenase, [NiFe]-hydrogenase and methyl-*S*-coenzyme-M methylreductase are known to contain nickel centers, which are intimately involved in the catalytic cycles[9].

†Presented to the National Conference on Chemistry Solutions at SRM University, India

Experimental

Elemental Analysis of the complexes is obtained using a Haereus CHN rapid analyzer. Conductivity measurement of the complexes is obtained using a Elico digital conductivity bridge modal CM-88 using freshly prepared solution of the complex in DMF. IR spectra were recorded on a PerkinElmer FT-IR 8300 series spectrophotometer on KBr disks from 4000 to 400 cm^{-1}. ^{1}H NMR spectra were recorded using a BRUKER GSX 300MHz NMR spectrometer. Mass spectra were obtained on a JEOL DX-303 mass spectrometer. Electronic spectral studies were carried out on a PerkinElmer 320 spectrophotometer from 200 to 1100 nm. Cyclic voltammograms were obtained on a CHI-600A electrochemical analyzer under oxygen-free conditions using a three-electrode cell in which a glassy carbon electrode was the working electrode, a saturated Ag/AgCl electrode was the reference electrode and platinum wire was the auxiliary electrode. A ferrocene/ ferrocenium couple was used as an internal standard and $E_{1/2}$ of the ferrocene/ ferrocenium (Fc/Fc^{+}) couple under the experimental condition was 470 mV. Tetra(*n*-butyl)ammonium perchlorate (TBAP) was used as the supporting electrolyte. Room temperature magnetic moments were measured on a PAR vibrating sample magnetometer Model- 155. X-band EPR spectra were recorded at 25 ºC on a Varian EPR-E 112 spectrometer using diphenylpicrylhydrazine (DPPH) as the reference. Catalytic oxidation of catechol to o-quinone by the copper complexes was studied in 10^{-3} M dimethylformamide solutions. The reactions were followed spectrophotometrically with the strongest absorption band of *o*-quinone at 390 nm and monitoring the increase in absorbance. A plot of log $(A_\infty/A_\infty-A_t)$ *vs.* time was made for each complex and the rate constant for the catalytic oxidations were calculated.

Chemicals and reagent

5-Bromosalicylaldehyde was purchased from Sigma-Aldrich. Analytical grade ethanol, acetonitrile, and DMF were purchased from Qualigens. TBAP, used as supporting electrolyte in electrochemical measurements, was purchased from Fluka and recrystallized from hot methanol. *N,N*-bis-(3-aminopropyl) piperazine, *N,N*-bis-(3-aminopropyl) ethylene diamine and tris-(2-aminoethyl)amine were purchased from Aldrich. Triethylenetetramine and diethylenetriamine were purchased from Qualigens.

Microorganisms

The test bacterial strains *Pseudomonas aeruginosa*, *E.coli, Candida albicans* and *Salmonella typhii* were obtained from the Department of Microbiology, SRM Medical University, Chennai, Tamil Nadu was isolated clinically. The test organisms were sub-cultured at 37 °C and maintained on nutrient agar media.

Disc diffusion method

The bacterial inoculum was uniformly spread using sterile glass rod on a sterile Petri dish containing Nutrient Agar. Five concentrations of 25, 50, 75, 100 and 125 µM of pure substances were prepared in DMSO. The test substances of 50 µL were added to each of the 5 wells (7 mm diameter holes cut in the agar gel, 20 mm apart from one another). The systems were incubated for 24 h at 36 ºC ±1 ºC, under aerobic conditions. After incubation, confluent bacterial growth was observed. Inhibition of the bacterial growth was measured in mm. Tests were performed in duplicate, whose minimum inhibitory concentration (MIC) values are provided in centimeters (cm) in diameter.

General synthesis of ligands

Synthesis of (9E)-N^1-(2-hydroxy-5-bromobenzylidene)-N^2-((E)-2-(2-hydroxy-5-bromo benzylideneamino)ethyl)ethane-1,2-diamine[L^1]

An absolute methanol solution (10 mL) containing diethylenetriamine (0.1030 g, 1 mmol) was added drop-wise to a stirred solution of 5-bromosalicylaldehyde (0.4020 g, 2 mmol). The solution was refluxed for 8 hours the above reaction shown in Scheme 1. The resulting yellow solution was cooled in ice. The yellow precipitate formed was filtered and washed with hexane and dried under vacuum. The crude product on recrystallization from THF gave yellow crystals.

Yield (53.8%). M.p.: 156 °C. Anal. For Analy. For $C_{18}H_{19}Br_2N_3O_2$; Calcd(%): C, 46.08; H, 4.08; N, 8.96; Found C, 46.04; H, 4.05; N, 8.91; ESI MS: (*m/z*) 467.19 [MH$^+$]. Calcd av. *m/z* 466.98. IR data, (KBr)(ν, cm^{-1}): 3385 ν [b,(OH)],1625 [s, ν(C=N)], ^{1}H NMR (ppm in CDCl$_3$ 300 MHz): δ 2.93(t, 2H, J = 5.4 Hz), 3.65 (t, 2H, J = 5.4 Hz), 6.74–7.32(m, 3H), 8.21 (s, 1H), 13.27(s,1H). ^{13}C NMR (CDCl$_3$, 300MHz): δ 46.31, 53.21, 117.27, 119.52, 126.28, 138.71, 139.11, 161.71, 162.31.

Ligands L^2, L^3, L^4 and L^5 were synthesized by following the above procedure using tris-(2-aminoethyl)amine (0.1490 g,1 mmol), triethylenetetramine (0.1420 g,1 mmol), *N,N*-bis-(3-aminopropyl)ethylenediamine (0.1740 g,1 mmol) and *N,N*-bis-(3-aminopropyl)piperazine (0.2000 g, 1 mmol) respectively instead of diethylenetriamine.

Synthesis of N^1,N^1-bis((E)-2-(2-hydroxy5-bromobenzylideneamino)ethyl)ethane-1,2-diamine [L^2]

Yield (33.2%). M.p.: 148 °C. Anal. For $C_{20}H_{24}Br_2N_4O_2$;Calcd (%): C, 46.89; H, 4.72; N, 10.94; Found C, 46.87; H, 4.70; N, 10.92; ESI MS: (*m/z*) 510.03Calcd av. *m/z* 512.24 selected IR data (KBr) (ν, cm^{-1}): 3471[b, ν(OH)], 1632[s, ν(C=N)], ^{1}H NMR (ppm in CDCl$_3$ 300 MHz): δ 2.07 (s, 2H), 2.5–12.59 (m, 8H), 3.71 (m, 4H), 8.32 (s, 2H), 6.53–7.80 (m, 6H), 8.14 (s, 2H). ^{13}C NMR (CDCl$_3$,300MHz): δ 39.23, 52.57, 58.14, 59.03, 117.08, 118.32, 126.07, 133.75, 137.07, 163.13, 164.41.

Synthesis of (9E)-N^1-(2-((E)-2-(2-hydroxy-5-bromobenzylideneamino)ethylamino) ethyl)-N^2-(2-hydroxy-5-bromobenzylidene)ethane-1,2-diamine [L^3]

Yield (39.5%). M.p.: 135 °C. Anal.for $C_{20}H_{24}Br_2N_4O_2$;Calcd (%): C, 46.89; H, 4.72; N, 10.94; Found C, 46.86; H, 4.68; N, 10.92; ESI MS: (*m/z*) 510.03 [MH$^+$]. Calcd av. *m/z* 512.67. Selected IR data (KBr) (ν, cm^{-1}): 3443 ν(OH), 1620[s, ν(C=N)], ^{1}H NMR (ppm in CDCl$_3$ 300 MHz): δ 2.94 – 3.02 (m, 4H), 3.41 – 3.47 (m, 4H), 2.67–2.86 (m, 4H), 6.64–7.41 (m, 6H), 7.41 (s, 2H), 13.17 (s, 2H) : ^{13}C NMR (CDCl$_3$,300MHz): δ 49.70, 52.93, 58.35, 110.73, 115.43, 130.21, 137.23, 138.61, 163.26, 164.14.

Synthesis of (9E)-N^1-(2-((E)-3-(2-hydroxy-5-bromobenzylideneamino)propylamino) ethyl)-N^3-(2,5-dibromobenzylidene)propane-1,3-diamine [L^4]

Yield (31.5%). M.p.: 140 °C. Anal. For $C_{22}H_{28}Br_2N_4O_2$;Calcd (%): C, 48.91; H, 5.22; N, 10.37; Found C, 48.88; H, 5.20; N, 10.34; ESI MS: (*m/z*) 541.30, Calcd av. *m/z* 540.29 selected IR data (KBr) (ν, cm^{-1}): 3465 ν(OH), 1630 [s, ν(C=N)]. ^{1}H NMR (ppm in CDCl$_3$ 300 MHz): δ 1.71–1.78 (m, 4H), 2.53–2.67 (m, 4H) 2.13–2.24 (m, 4H), 3.48 (t, 4H, J=6.2 Hz), 6.63–7.82 (m, 6H), 8.44 (s, 2H), 8.12(s, 2H), 12.41 (s, 2H) ^{13}C NMR (CDCl$_3$,300MHz) : 32.17, 37.27, 38.17, 116,62, 127.13, 132.51, 136.43,163.21, 165.11.

Synthesis of (9E)-N-(2-hydroxy-5-bromobenzylidene)-3-(4-((E)-3-(2-hydroxy-5-bromobenzylideneamino)propyl)piperazin-1-yl)propan-1-amine [L⁵]

Yield (34.5%). m.p.: 145 °C. Anal. for $C_{24}H_{30}Br_2N_4O_2$;Calcd (%): C, 50.90; H, 5.34; N, 9.89; Found :C, 50.87; H, 5.32; N, 9.87; ESI MS: (*m/z*) 563.33Calcd av. *m/z* 566.33 selected IR data (KBr) (ν, cm⁻¹): 3465ν(OH), 1622 [s, ν(C=N)]. ¹H NMR (ppm in CDCl₃ 300 MHz): δ 1.96–2.00 (m, 4H), 2.55–2.59(m,4H), 2.60–2.68 (m, 8H), 3.67–3.71 (m, 4H) 6.85–7.41 (m, 6H), 13.48 (s, 2H) (CDCl₃,300MHz): δ 29.42, 52.63, 55.23, 68.71, 118.23, 119.28, 128.23, 132.21, 137.82, 157.33, 159.92.

Synthesis of nickel complex

Synthesis of mono nuclear [Ni(II)L¹(ClO₄)] complex

An absolute methanol solution containing Ni(ClO₄)₂.6H₂O (0.0365 g, 0.1 mmol) was added drop wise to a stirring solution of L¹ (0.0466 g, 0.1 mmol) in 20 mL of absolute methanol. The solution was refluxed for 8 hours the above reaction shown in Scheme 2. On cooling the solution yellow color microcrystals are formed, which were filtered and washed with methanol followed by diethyl ether and dried in vacuum. The crude product was recrystallized from methanol and acetonitrile (1:3, v/v). [Ni(II)L²], [Ni(II)L³], [Ni(II)L⁴] and [Ni(II)L⁵] were synthesis by following the above procedure using L² (0.0512 g, 0.1 mmol), L³ (0.0512 g, 0.1 mmol), L⁴(0.0540 g, 0.1 mmol) and L⁵(0.0566 g, 0.1 mmol) ligands (Scheme 1).
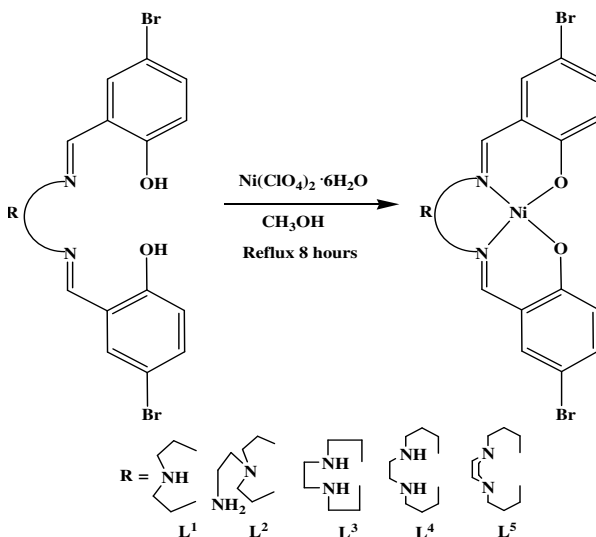
Scheme 1

Yield: (59%) m.p.:321 °C (dec). Anal.for $C_{18}H_{16}Br_2ClN_3O_6Ni$; Calcd (%): C, 34.63; H, 2.58; N, 6.73; Ni, 9.40; Found (%): C, 34.60; H, 2.56; N, 6.71; Ni, 9.38; ESI Mass: (*m/z* 622.84 Calcd av. *m/z* 624.29). Conductance (*Λ* Scm² mol⁻¹) in DMF: 129. Selected IR data (KBr) (ν, cm⁻¹): 3360 b [ν (N-CH₂)], 1634 s [ν(C=N)], 1087 w [ν (ClO₄⁻) coordinated], 611 s [ν (M-N)], 430 m [ν (M-O)].

Synthesis of [Ni(II)L²]Complex

Yield: (66%) m.p.:284 °C (dec). Anal.for $C_{20}H_{22}Br_2N_4O_2$ Ni; Calcd (%):C, 42.30; H, 3.73;N, 9.87; Ni, 10.34; Found (%):C, 42.28; H, 3.71;N, 9.86; Ni, 10.32;ESI Mass: (*m/z* 565.96 Calcd

av. *m/z* 568.92). Conductance (Λ Scm^2 mol^{-1}) in DMF: 55. Selected IR data (KBr) (v, cm^{-1}): 3173 v (N-CH$_2$), 1623 [s, v(C=N)], 629 [s, v (M-N)], 482 [s, v (M-O)].

Synthesis of [Ni(II)L^3] complex

Yield: (52%) m.p.:225 °C (dec). Anal.for C$_{20}$H$_{20}$Br$_2$N$_4$O$_2$Ni; Calcd (%): C, 42.37; H, 3.56; N, 9.88; Ni, 10.35; Found (%): C, 42.34; H, 3.54; N, 9.86; Ni, 10.32; ESI Mass: (*m/z* 564.94Calcd av. *m/z* 566.90). Conductance (Λ Scm^2 mol^{-1}) in DMF: 59. Selected IR data (KBr) (v, cm^{-1}): 3224 v (N-CH$_2$), 1636 [s, v(C=N)], 598 [s, v (M-N)], 467 [s, v (M-O)].

Synthesis of [Ni(II)L^4] complex

Yield: (57%) m.p.:224 °C (dec). Anal.for C$_{22}$H$_{24}$Br$_2$N$_4$O$_2$Ni; Calcd (%): C, 44.41; H, 4.07;N, 9.42; Ni, 9.87; Found (%): C, 44.39; H, 4.00;N, 9.40; Ni, 9.86; ESI Mass: (*m/z* 592.93 Calcd av. *m/z* 594.95).Conductance (Λ Scm^2 mol^{-1}) in DMF: 51. Selected IR data (KBr) (v, cm^{-1}): 3119 v (N-CH$_2$), 1629 [s, v(C=N)], 589 [s, v (M-N)], 488 [s, v (M-O)].

Synthesis of [Ni(II)L^5] complex

Yield: (54%) m.p.: 225 °C (dec). Anal.for C$_{24}$H$_{28}$Br$_2$N$_4$O$_2$Ni; Calcd (%):C, 46.27; H, 4.53; N, 8.99; Ni, 9.42; Found (%):C, 46.25; H, 4.52; N, 8.97; Ni, 9.40; ESI Mass: (*m/z* 621.93Calcd av. *m/z* 623.01).Conductance (Λ Scm^2 mol^{-1}) in DMF: 56. Selected IR data (KBr) (v, cm^{-1}): 3134 v (N-CH$_2$), 1635 [s, v(C=N)], 597 [s, v (M-N)], 487 [s, v (M-O)].

Results and Discussion

FT IR spectral analysis

The FT IR spectrum of the precursor compound (PC) shows a sharp band at around 1668 cm^{-1} due to the presence of CHO group. The OH group in the ligand shows a broad peak at 3378 cm^{-1}. All the ligands show a band at 3389 cm^{-1} due to the phenolic and aliphatic OH groups. The band in the region of 1636- 1590 cm^{-1} in the ligands is due to the presence of imine (C=N) group. All the complexes show a sharp band in the region 1636 – 1620 cm^{-1}, due to v(C=N) stretching. The complete disappearance of aldehydic group of the precursor and the appearance of imine (CH=N-) group in the ligands show the effective Schiff base condensation between the aldehyde group of the precursor compound and the amine groups[10]. For the complexes, bands at 460–490 cm^{-1} could be assigned to –M–O bond. Other weak bands at lower frequency could be assigned to –M–N bond[11]. The spectra of all the complexes are dominated by bands at 3150-3070 cm^{-1} due to the aromatic C-H stretching vibration. A strong band at 1260 cm^{-1} in the free Schiff bases has been assigned to phenolic C–O stretching vibration. Upon complexation, this band shifts to higher frequency (1300 cm^{-1}) showing coordination through phenolic oxygen[12]. The presence of uncoordinated perchlorate anions in all of the mononuclear complexes are inferred from a single broad band around 1100 cm^{-1} (v$_3$-antisymmetric stretching) which are not split and a band around 650 cm^{-1} (v$_4$-antisymmetric bending). The band around 930 cm^{-1} (v$_2$- symmetric stretching) due to coordinated perchlorate is not observed and this indicates that no perchlorate ions are coordinated in the complexes.

Electronic spectra

Electronic spectra of all the complexes were obtained in DMF medium. The electronic absorption spectra of Ni(II) complexes are recorded at 25 °C and the absorption region assignment data are given in Table 1 and the proposed geometry of the complexes are given.
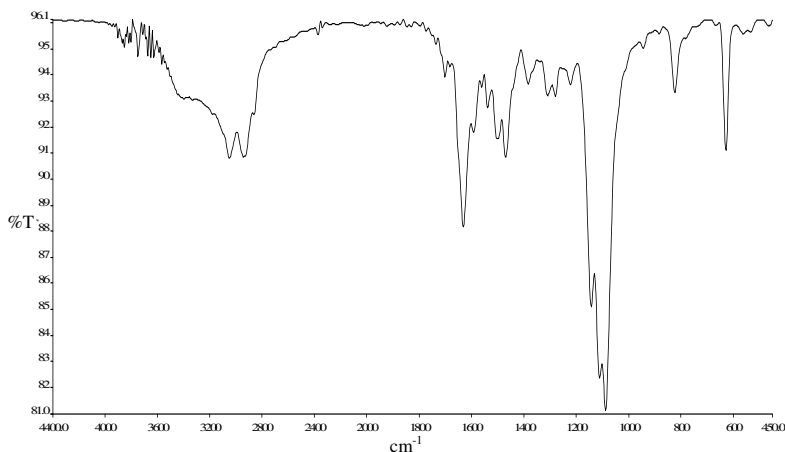
**Figure 1.** FT IR spectrum of: [NiL^1(ClO$_4$)] complex

Table 1. Electronic spectral data of acyclic mononuclear [Ni(II)L$^{1-5}$] complexes

Sl. No.	Complexes	λ_{max}, nm, ε/M^{-1} cm^{-1}		
		d-d	Charge transfer	
1.	[Ni(II)L^1(ClO$_4$)]	780(125)	330(19409)	305 (21342)
2.	[Ni(II)L^2]	791(123)	335(19335)	302 (21287)
3.	[Ni(II)L^3]	825(116)	370(16965)	280 (22654)
4.	[Ni(II)L^4]	843(109)	375(16841)	270 (24137)
5.	[Ni(II)L^5]	920(96)	386(16221)	267 (24272)

The electronic spectra of [Ni(II)L] complexes show a single weak d-d band in region 780-832 nm due to $^3A_2 \rightarrow {}^3T_2(F)$, $^3T_1(F)$ associated with distorted octahedral geometry[13]. A red shift in the λ_{max} value of d-d band[14] with increase in the chain length between imine nitrogen has been observed. This red shift may be due to the distortion from planar geometry as the chain length increases. Moderately intense band observed in the region of 365-385 nm is associated with ligand to metal charge transfer transition. An intense band observed in the region 280-305 nm is associated with intra ligands transition. The electronic absorption spectra are given in Figure 2 & 3.
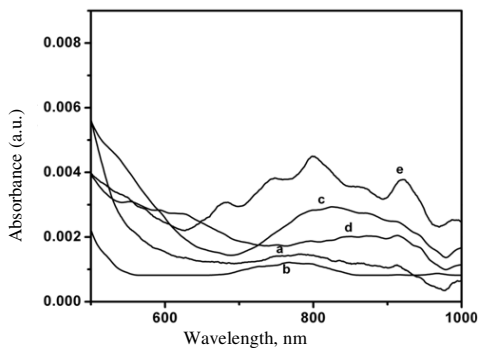
Figure 2. Electronic spectra of (a) [NiL^1(ClO$_4$)]; (b) [NiL^2]; (c) [NiL^3]; (d) [NiL^4] and (e) [NiL^5]
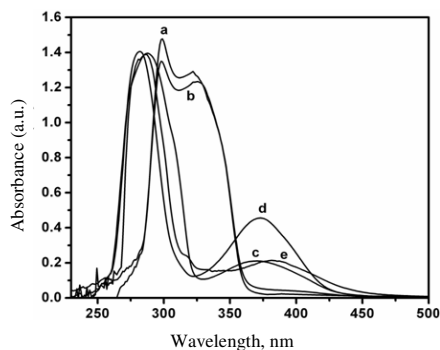
**Figure 3.** Electronic spectra of (a) [NiL^1(ClO$_4$)]; (b) [NiL^2]; (c) [NiL^3]; (d) [NiL^4] and (e) [NiL^5]

**Electrochemistry of the nickel(II) complexes**

Reduction process at negative potential

The electrochemical behavior of [Ni(II)L] complexesare given in Figure 4. The reduction potential shifts towards anodic direction for the complexes [Ni(II)L^1(ClO$_4$)] to [Ni(II)L^5] from -1.23 V to -0.90 V, as the number of methylene groups increases. This shows that, as the number of methylene groups between the imine nitrogen (chain length) increases, the entire acyclic ring becomes more flexible, which causes a distortion of the geometry of the nickel(II) complexes and makes the system more flexible, which stabilizes the low valent Ni(I).

Oxidation process at positive potential

The oxidation potential shifts towards cathodic direction for the complexes [Ni(II)L^1] to [Ni(II)L^5] from 0.45 V to 0.68 V as the number of methylene group is increased. The cyclic voltammograms are given in Figure 5. This is because, as the ring size increases the flexibility and the planarity of the complexes decreases and the electrochemical oxidation process occurs with difficult.
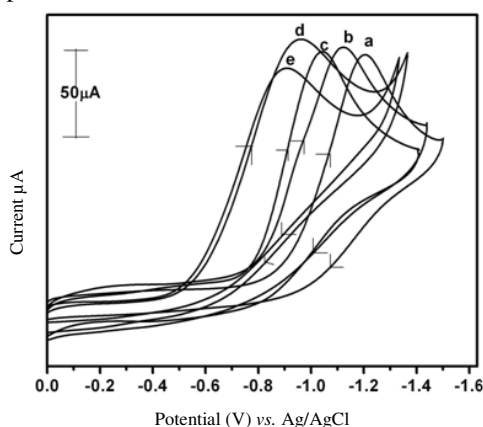
Figure 4. Cyclic voltammogram of (a) [NiL^1 (ClO$_4$)]; (b) [NiL^2]; (c) [NiL^3]; (d) [NiL^4] and (e) [NiL^5].
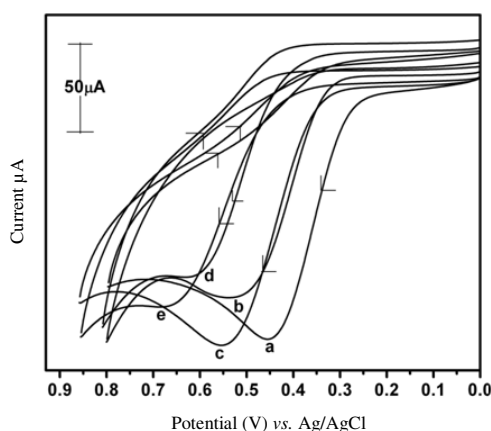
Figure 5. Cyclic voltammogram of (a) [NiL^1 (ClO$_4$)]; (b) [NiL^2]; (c) [NiL^3]; (d) [NiL^4] and (e) [NiL^5].

Table 2. Electrochemical data and rate constant for hydrolysis of 4-nitrophenylphosphate for [Ni(II)L$^{1-5}$] complexes

No	Complexes	[a]Reduction (at cathodic) (V) Potential	[a]Oxidation (at anodic) (V) Potential	[b]Rate constant (k) × 10^{-3} min^{-1} NPP
1	[Ni(II)L^1(ClO)$_4$]	-1.23	0.45	1.85
2	[Ni(II)L^2]	-1.13	0.53	2.84
3	[Ni(II)L^3]	-1.05	0.55	4.39
4	[Ni(II)L$_4$]	-0.95	0.60	6.86
5	[Ni(II)L^5]	-0.90	0.68	8.37

[a]*Measured by CV at 50 mv/s. E vs Ag/AgCl ; Condition: GC working electrode and Ag/AgCl Reference electrode: supporting electrolyte TBAP, concentration of complexes 1×10^{-1}M.*
[b]*Measured spectrophotometrically in DMF, concentration of the complexes: 1×10^{-3}M*

Kinetic studies of hydrolysis of 4-nitrophenylphosphate

The catalytic activity of the nickel(II) complexes on thehydrolysis of 4-nitrophenyl-phosphate was determined spectrophotometrically by monitoring the increase in the characteristicabsorbance of the 4-nitrophenolate anion at420 nm over the time in dimethylformamide at 25 °C. For this purpose, 10^{-3} mol dm^{-3} solutions of complexes in dimethylformamide were treated with 100 equivalents of 4-nitrophenyl phosphate in the presence of air. The course of the reaction was followed at 420 nm regular time intervals (40 min.). The slope was determined by the method of initial rates by monitoring the growth of the 420 nm band of the product 4-nitrophenolate anion. A linear relationship for all the complexes shows a first-order dependence on the complex concentration for the systems. Plots of log $(A_{\infty}/A_{\infty}-A_t)$ versus time for hydrolysis of 4-nitrophenylphosphate activity of the complexes are obtained and shown in Figure 6. The inset in Figure 6 shows the time dependent growth of *p*-nitrophenolate chromophore in the presence of [Ni(II)L^5]. The catalytic activities of the nickel(II) complexes are founded to increase as the chain length increases due to the flexibility resulting from the distraction of the coordination sphere, *i.e*. increasing in the chain length enhances the rate constant of hydrolysis fairly well by producing distortion in the geometry around the metal ion that enhances the accessibility of the metal ion for the bonding of phosphate and OH group[15]. The rate constant value for the mononuclear nickel(II) complex [Ni(II)L^5] is higher (8.37×10^{-3} min^{-1}) than that of the complex [Ni(II)L^4] (6.86×10^{-3} min^{-1}) which in turn is higher than the nickel(II) complex [Ni(II)L^1] (1.85×10^{-3} min^{-1}).
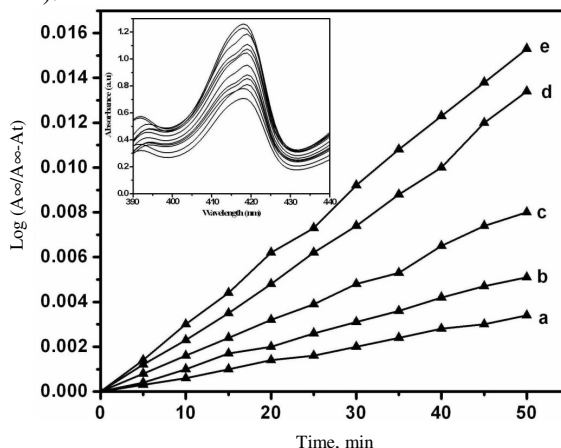
Figure 6. Hydrolysis of 4-nitrophenylphosphate by (a) [NiL^1(ClO$_4$)]; (b) [NiL^2]; (c) [NiL^3]; (d) [NiL^4] and (e) [NiL^5] The inset is the time dependent growth of *p*-nitrophenolate chromophore in the presence of [NiL^5]

Antimicrobial activity

Antimicrobial activity of synthesized nickel(II) complexes against five tested microorganisms has been studied. As per the recorded data all the mono nuclear compounds showed different effects against the different organisms.The nickel(II) complexes showing highest activity against *Salmonellaq typhii* and at the concentration of 125 µM. Complex [Ni(II)L^5] has the highest antimicrobial activity against all the organisms, in contrast [Ni(II)L^2] showed the lowest activity. This difference in inhibition may be due to the differences between the cell structures of bacteria, yeast and not depend upon the number of

alkyl group present in the complex. While the cell walls of fungi contain chitin, the cell walls of bacteria contain murein[16]. In addition, fungi contain ergosterol in their cell membranes instead of the cholesterol found in the cell membranes of animals[17]. In addition, the difference in the antibacterial activity nickel(II) complexes studied in this work.

Conclusion

In conclusion, five Schiff base nickel(II) complexes have been synthesized and their coordination chemistry and antibacterial activity have been investigated. The electronic spectra of $[Ni(II)L^{1-5}]$ complexes indicates square planar geometry and there is a red shift due to the increase in the chain length. Cyclic voltammograms exhibit one electron quasi-reversible process. The reduction potential shifts to more negative potential on increasing chain length and oxidation potential shifts more positive potential on increasing chain length. All the $[Ni(II)L^{1-5}]$ complexes show good catalytic activity on increasing the chain length. Increase in the chain length causes a greater distortion of the geometry of the complexes. This flexibility in the geometry may favour the observed higher rate of the reaction. The nickel(II) complexes showing highest activity against *Salmonellaq typhii* and at the concentration of 125 µM. Complex $[Ni(II)L^5]$ has the highest antimicrobial activity against all the organisms, All these studies of the complexes agree well with the established trend.

Reference

1. Adams H, Bucknal R M, Fenton D E, Rodríguez C O, García M and Oakes J, *Polyhedron*, 1998, **17(21)**, 3803-3808.
2. Hernandez Molina R and Mederos A, In Comprehensive Coordination Chemistry II, Ed., Lever A B P, Elsevier-Pergamon Press: New York, 2003, **1**, 411.
3. Mueller K and Schert U, Organic Light Emitting Devices; Wiley-WCH: New York, 2006.
4. Hadson S A and Maitlis P V, *Chem Rev.,* 1993, **93,** 861
5. Burdette S C and Lippard S J, *Coord Chem Rev.,* 2001, **216,** 333-361.
6. (a) Che C M and Huang J S, *Coord Chem Rev.,* 2003, **242,** 97-113; (b) Venkataraman N S, Kuppuraj G and Rajagopal S, *Coord Chem Rev.,* 2005, **249,** 1249.
7. Saleh A A, *J Coord Chem.,* 2005, **58,** 255.
8. Thauer R K, Diekert G and Schonheit P, *Trends Biochem Sci.,* 1980, **5,** 304.
9. (a) Halcrow M A and Christou G, *Chem Rev.,* 1994, **94,** 2421-2481; (b) Kolodziej A F, *Prog Inorg Chem.,* 1994, **41,** 493.
10. EI-Metwally N M, Gabr I M, Shallaby A M and EI-Asmy A A, *J Coord Chem.*, 2005, **58**, 1154.
11. Kaloyanov N, Neykor M, Wesselinova D W and Dimiltrov G D, *Cent Eur J Chem.,* 2012, **10,** 1034.
12. Nakamoto K, Infrared Spectra of Inorganic and Coordination Compounds; John Willey and Sons: New York, 1986, 244.
13. Raman N, Dhaveethu R J, Sakthivel A and Chil J, *Chem Soc.,* 2008, **53(3),** 1568-1571.
14. Bottcher A, Elias H, Jager E G, Langfelderova H, Mazur M, Muller L, Paulus H, P. Pelikan P, Rudolph M and Valko M, *Inorg Chem.,*.1993, **32**, 4131-4138.
15. Vijayaraj A, Prabu R, Suresh R, Jayanthi G, Muthumary J and Narayanan V, *Synthesis and Reactivity in Inorganic, Metal-Organic and Nano-Metal Chem.*, 2011, **41(8)**, 963-972.
16. Eweis M, Elkholy S.S and Elsabee M Z, *Int J Biol Macromol.*, 2006, **38**, 1-8.
17. Fleet G H, Composition and Structure of Yeast Cell Walls Current Topics in Medical Mycology, Springer-Verlag: New York USA, Vol 1, 1985.